Modeling Earth Systems and Environment (2024) 10:2957–2975
https://doi.org/10.1007/s40808-023-01937-6

ORIGINAL ARTICLE

Modeling future (2021–2050) meteorological drought characteristics using CMIP6 climate scenarios in the Western Cape Province, South Africa

Mthulisi Ngwenya[1] · **Mulala Danny Simatele**[1]

Received: 1 November 2023 / Accepted: 16 December 2023 / Published online: 2 February 2024

Abstract
Consistent drought modelling under plausible shared socioeconomic–representative concentration pathways (SSP–RCPs) are crucial for effectively managing future drought risk in agricultural environments. The Western Cape (WC) is one of South Africa's main agro-based provinces and faces a mounting threat of water insecurity due to recurrent drought. The objective of this study was to predict meteorological drought hazard for 2021–2050 based on three CMIP6 scenarios: SSP5–8.5, SSP2–4.5 and SSP1–2.6. Precipitation simulations generated by the sixth version of Model for Interdisciplinary Research on Climate (MIROC6) under the SSP5–8.5, SSP2–4.5 and SSP1–2.6 scenarios were used from fifteen stations across the six AEZs of the WC province. The Standardised Precipitation Index (SPI) was computed at 12-month timescales. Trend analysis of precipitation datasets and the SPI-values were done at $p < 0.05$ using the Mann–Kendall (M–K) test. The findings revealed negative precipitation trends of −7.6 mm/year in Ceres, while positive trends of 0.3 mm/year were observed in Malmesbury. These findings indicate an improvement from −7.8 and −6.4 mm/year in the same regions, respectively, compared to historical trends observed between 1980 and 2020. The results suggest that in 2042 and 2044, Bredasdorp will experience $-2 < SPI < -1.5$ under the SSP2–4.5 scenarios, while Matroosberg in 2038 under the SSP5–8.5 will experience $SPI > -2$. The findings of this study will assist in the development of proactive planning and implementation of drought mitigation strategies and policies aimed at reducing water insecurity in AEZs.

Keywords Drought prediction · Statistical downscaling · SPI · CMIP6 · Western Cape, South Africa

Introduction

Drought is one of the deadliest natural hazards that fundamentally occurs in all regions of the world (Hao et al. 2018). Drought occurs when the amount of water in soils, streams, reservoirs, and aquifers is inadequate to meet society's and the environment's needs (Vicente-Serrano et al. 2022). Gergis and Henley (2017) argued that drought is characterised by periods of deficient precipitation and, if it continues over extended periods, leads to severe social, environmental and economic impacts in affected regions. Gidey et al. (2018) argued that the impacts of drought are evident through chronic water shortages and ultimately slowing down agricultural production. Vicente-Serrano et al. (2022) noted that the global economic losses from drought incidence between 2000 and 2015 were reported to be over $600 billion United States dollars (USD). This global trend towards more severe drought conditions has mainly been more severe in developing countries in sub-Saharan Africa that rely heavily on rainfed agriculture due to their low adaptive capacities (Okunola et al. 2023). For instance, Engelbrecht and Monteiro (2021) argued that the greatest threat to sustainable development in South Africa in the near term (2021–2040) is one or more extreme droughts occurring. Recurrent droughts are particularly concerning, considering that most of South Africa's agricultural production regions rely on rainfed agriculture to meet the rising global demand for food (Mugejo et al. 2022). One region that has been tremendously affected by the impacts of drought in South Africa is the Western Cape Province (Calverley and Walther 2022). The Western Cape Province was hardest hit by the worst inter-annual drought

✉ Mthulisi Ngwenya
2463724@students.wits.ac.za

[1] School of Geography, Archaeology and Environmental Studies, University of the Witwatersrand, Johannesburg, South Africa

since 1904 between 2015 and 2017, which resulted in unprecedented water shortages that led authorities to suggest the implementation of 'Day Zero' where household water-use would be temporarily suspended (Ndebele et al. 2020).

Numerous scholars, such as Lange et al. (2020) and Tapiador et al. (2020), have suggested that monitoring and evaluating future characteristics of hydroclimatic variability together with shared socioeconomic pathways–representative concentration pathways (RCP–SSPs) is vital for modelling future drought characteristics and their impacts on water security. However, recent advancements in climate projections and drought prediction have remained sophisticated and largely limited (Hao et al. 2018), partly due to uncertainties in climate data simulations (Basak et al. 2022). Poornima and Pushpalatha (2019) argued that the only scientifically acceptable technique for modelling future drought characteristics has been through the use of Global Climate Model (GCM) projections developed under the Coupled Model Intercomparison Projects (CMIP). The Intergovernmental Panel on Climate Change Sixth Assessment Report (IPCC, AR6) recently unveiled the Coupled Model Intercomparison Project Phase 6 (CMIP6) to investigate and compare climate projections made from coupled ocean–atmosphere–cryosphere–land GCMs (Meehl et al. 2000). The CMIP6 framework couples plausible future representative concentration pathways (RCPs) with alternative shared socioeconomic pathways (SSPs) in order to research climate change impacts, adaptation, and mitigation (Eyring et al. 2019). Rogelj et al. (2012) noted that the CMIP6 framework applies a combination of four plausible climate change scenarios, namely SSP1–2.6, SSP2–4.5, SSP3–7.0 and SSP5–8.5 to monitor future drought characteristics.

O'Neill et al. (2017) suggested that plausible climate change scenarios constitute an essential component of climate change impact as they aid researchers and decision-makers in understanding the consequences of near- and long-term climate changes. The SSP1–2.6 model describes the low extreme limit of the range of projected scenarios and apprises the RCP2.6 scenario (Tebaldi et al. 2021). The SSP2–4.5 model describes the intermediate portion of the range of projected scenarios and revises the RCP4.5 scenario (Peng et al. 2023). The SP3–7.0 scenario is in the upper–middle part of the full range of scenarios. It was newly introduced after the RCP scenarios, closing the gap between RCP6.0 and RCP8.5 (Tan and Duan 2017). The SSP5–8.5 model characterises the high extreme limit of the range of projected scenarios (Zelinka et al. 2020). Mirgol et al. (2021) argued that climate change alternative scenarios, together with GCMs, enable water resource managers to predict the impacts of drought in the face of future global climate uncertainties. Vicente-Serrano et al. (2022) noted that the SSP–RCP climate change scenarios from CMIP6 permit for risk impact assessment of potential mitigation and adaptation strategies in natural resources climate management and societal transformation consistently.

Although GCM simulations underpinned by the CMIP6 framework present an excellent methodology to model the climate change impacts, it is widely accepted that GCM output has a very coarse resolution compared to that at which anthropological activities in a region of interest occur (Zelinka et al. 2020). Gupta et al. (2020) argued that GCM simulated datasets have a coarse spatial resolution (usually 500 kms grid cell), which is more significant than necessary for use in the more regional and local-based basins that require up to a minimum of 20-kilometres (km) grid cells. Scholars such as Huo-Po et al. (2013) and Tebaldi et al. (2021) have suggested that GCM simulations require downscaling to obtain output that can be used at regional and local scales. Downscaling bridges the gap between global yet coarse predictions and practical needs such as precipitation projection for hydrologic operations in local basins under climate change (Tapiador et al. 2020). Mirgol et al. (2021) highlighted that downscaling procedures have evolved to be an effective way of linking GCM simulations (frequently atmospheric circulation data) to local scale surface variables (such as precipitation). Christensen et al. (2007) reported that two types of downscaling techniques are available: dynamic downscaling (DD) and statistical downscaling (SD).

Spinoni et al. (2020) noted that DD involves the use of high-resolution regional climate model (RCM) simulations to extrapolate the impacts of large-scale climate processes to regions or local scales of interest. The resolution in most RCMs ranges from 20 to 60 km (Stefanidis et al. 2020). Due to its high computing cost, DD has minimal application in impact studies and is only helpful for local scale simulations (Burke et al. 2006). Salvi et al. (2011) argued that DD is complicated and demands the same computing power as GCM simulations. Rashid et al. (2017) noted that DD is difficult to execute accurately and is primarily used to process GCM projection to better resolution RCM output. On the other hand, SD techniques are more efficient than DD techniques and are widely used due to their structural simplicity (Iizumi et al. 2011). One of the many benefits of using SD techniques is that compared to the DD technique, they require less computations and may be applied to downscale many GCM climate simulations (Sachindra et al. 2014). Fowler et al. (2007) noted that SD techniques offer local-scale climate information from GCM climate projections. Broadly, SD approaches can be further categorised into three classes: transfer function method (Ding et al. 2019), weather typing (Richardson 1981) and weather pattern schemes (Qin et al. 2021). The Bias Correction (BC) underpinned by the transfer function method has been primarily adopted and widely applied in climate change studies for downscaling purposes (Salvi et al. 2011).

Zhang et al. (2021) noted that in order to predict drought characteristics credibly, a suitable drought index should be selected. While numerous drought monitoring indices are applied for drought characterisation, contradictory findings on their characteristics have been published, partly due to embedded constraints in the numerous drought monitoring indices (Um et al. 2022). The use of these indices is location-specific due to the dynamic and evolutionary characteristics of drought environments. Amongst these numerous drought monitoring indices, the most widely used ones include the Palmer Drought Severity Index (PDSI) (Palmer 1965), Soil Moisture Index (SMI) (Wetherald and Manabe 2002), and the Standardised Precipitation Index (SPI) (McKee et al. 1993). For example, the PDSI is extensively applied in North America and quantifies the cumulative spatio-temporal deviation of moisture supply across space and time. It applies the Thornwaite's method of estimating potential evapotranspiration. However, the PDSI has restricted precision due to PET estimation's existential complexity and uncertainty, mostly in extreme climate conditions and mountainous regions. On the other hand, the SMI was developed to evaluate the quantity of water accessible by crops in the soil. The SMI index needs an assortment of climate data such as precipitation, temperature, potential evapotranspiration, and plant data such as vegetation type, leaf area, and management practices. The SPI is based on a probabilistic methodology that uses precipitation as the only input and has been widely adopted in recent decades as the drought index of choice over other indices due to its ability to be computed at multiple timescales (1-, 3-, 6-, 12-, 18-, and 24-month's) and capacity to differentiate between agricultural, meteorological and hydrological drought types (Hayes et al. 2011).

To this end, various scholars such as Kelley et al. (2015), Ndebele et al. (2020), and Engelbrecht and Monteiro (2021) concur that the pervasive and costly nature of drought remains the single greatest threat to water resources and agricultural production particularly in drought-prone regions such as the WC province of South Africa that rely on rainfed agriculture. Whilst several studies have investigated the probable impacts of climate change-induced drought on water resources, their investigations have been aimed at the catchment level (Kusangaya et al. 2014). For example, research conducted by Li et al. (2015) revealed that the impact of climate change in humid tropical zones of southern Africa caused some changes in the spatio-temporal distribution of observed precipitation. However, the study applied large-scale hydrological models that were underpinned by an RCM to examine the influence of climate change on hydrological elements such as evapotranspiration (ET) and surface runoff until 2029. Similarly, Graham et al. (2022) investigated the hydrological feedback to future climate change over the Thukela River Basin, South Africa. Their study revealed that future temperatures were predicted to increase in all scenarios, while there was no agreement on the impacts on water availability. The above study underscored the necessity for supplementary, reliable drought modelling studies in South Africa that seek to understand the future characteristics of drought better to manage the associated risk. More recently, using multi-model regional climate simulations from the Co-ordinated Regional Climate Downscaling Experiment (CORDEX), Abiodun et al. (2019) investigated the probable effects of climate change on droughts over four major basins in southern Africa. While the investigation looked into drought throughout southern Africa, it did not investigate climate change scenarios using the CMIP6 framework and was not localised in the Western Cape region in particular. Moreover, decisions on DEWS are usually undertaken at the provincial level, so there is an exigent requirement for new research at the provincial scale (Kusangaya et al. 2014).

Despite the WC province's high-water vulnerability to drought impacts, only a limited number of climate projections studies have been made for the region (Engelbrecht et al. 2013; Abiodun et al. 2019). Hence, this primary purpose of the study was to examine the potential impacts of meteorological drought on water resource availability in the WC province, an area especially vulnerable to climate change. The specific objectives of this study are to (i) downscale the three climate change scenario (SSP5–8.5, SSP2–4.5 and SSP1–2.6) datasets projected from the sixth version of Model for Interdisciplinary Research on Climate (MIROC6), (ii) evaluate the spatio-temporal characteristics of meteorological drought in the near-term period (2021–2050) under three projected scenarios (SSP5–8.5, SSP2–4.5 and SSP1–2.6) in the Western Cape Province of South Africa, and (iii) investigate the precipitation variability, projected drought duration, intensity, frequency, and spatial coverage of drought occurrences. This study has application in mitigating climate change impacts on future drought risk over South African river basins.

Materials and methods

Study area

The Western Cape (WC) Province in South Africa is found at the most southern tip of South Africa (Fig. 1). The province shares borders with the Eastern and Northern Capes, the Atlantic Ocean to the west, and the Indian Ocean to the south. The province experiences mild, wet winters and warm, dry summers due to its temperate Mediterranean climate. The average summer temperatures vary between 15 and 27 °C, and the average winter temperatures vary between 5 and 22 °C (Hurry and Van Heerden 1982; Tyson 1986; Kruger 2004). With only about 350 mm of mean

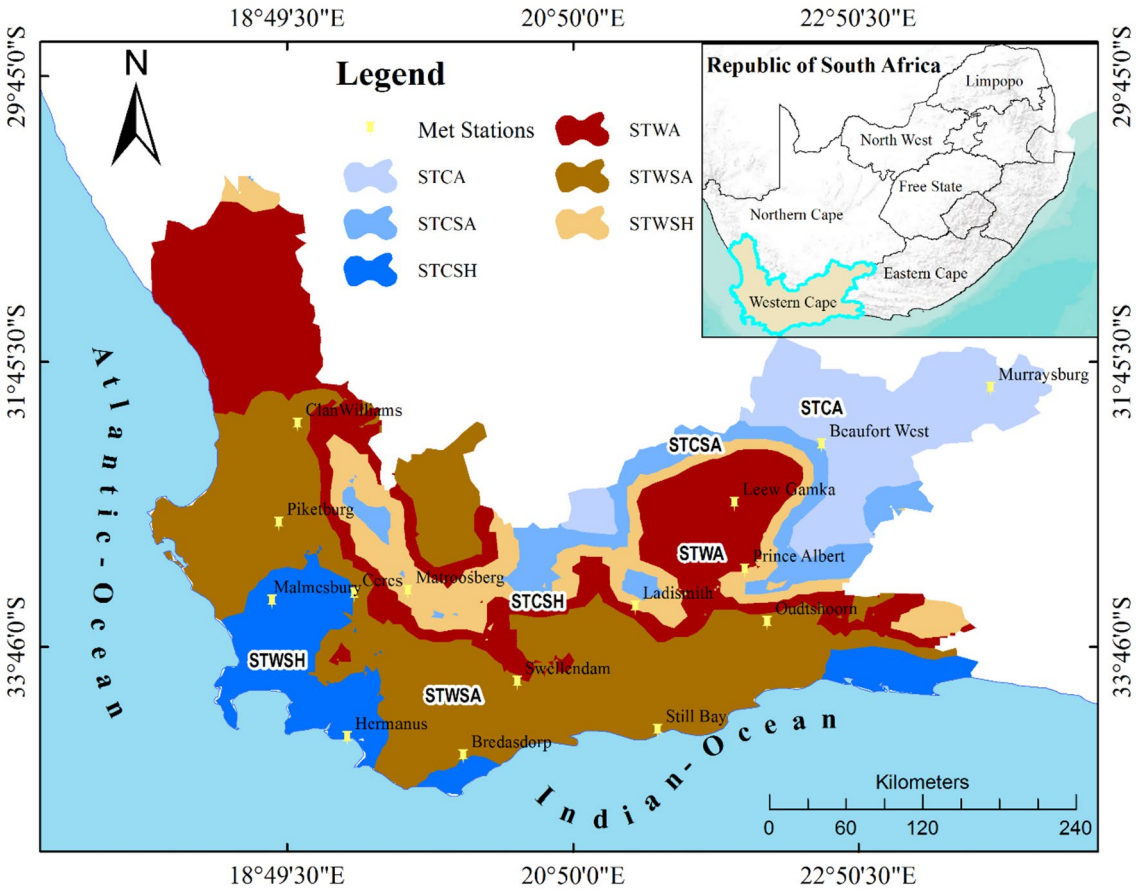

Fig. 1 Location of the study area (Adapted from Ngwenya et al. 2024)

annual precipitation (MAP), the WC province is one of the driest provinces in South Africa, receiving far less than the ~ 500 mm average for the entire country (Dennis and Dennis 2012). The austral winter months (between May and September) receive the majority of annual rainfall, which is usually brought on by extratropical cyclones and cold fronts, as well as sporadic westerly disturbances including cut-off lows. However, the distribution of rainfall is very varied, ranging from semi-arid regions to comparatively moist regions on the windward slopes of mountains (Blamey et al. 2017).The present study focuses on the six of South Africa's AEZs, that include subtropical warm/arid (STWA), subtropical cool arid (STCA), subtropical warm semi-arid (STWSA), subtropical cool/semi-arid (STCSA), subtropical warm subhumid (STWSH) and subtropical cool subhumid (STCSH). The AEZs are categorised based on the duration of the cropping season (Mugido and Shackleton 2017). Arid regions have a cropping season that last for 2 months; semi-arid regions have length of farming season ranging between 2 and 3 months; warm sub-humid regions have a cropping season of 3 to 4 months while cool sub-humid zones have a cropping season of 4 to 5 months (Muimba-Kankolongo 2018).

Data acquisition

Table 1 illustrates the selected meteorological stations used to acquire the daily observed, reanalysis and future precipitation datasets. Two forms of datasets were employed in the study: observational data and model simulations. Observed precipitation data (1980–2020), were gathered from the University of East Anglia's Climate Research Unit gridded Time Series (CRU TS Version 4.07) https://www.cru.uea.ac.uk/cru/data/hrg database using Google Earth engine interface, while future precipitation datasets (2021–2050) under SSP5–8.5, SSP2–4.5 and SSP1–2.6 climate scenarios were generated by https://esgf-node.llnl.gov/search/cmip6/ using the sixth version of Model for Interdisciplinary Research on Climate, (MIROC6). CRU TS Version 4.07 datasets have 0.5° by 0.5° resolution and are available across all regions except Antarctica (Harris et al. 2020). The spatial resolution of the precipitation data generated by the MIROC6 model is

Table 1 Location of stations in the Western Cape Province

Station	Location		Mean annual precipitation (MAP)	Temperature		Altitude (m)	AEZ
	Longitude (E)	Latitude (N)		Minimum temperature (°C)	Maximum temperature (°C)		
MG	23.8	−32.0	310.6	2.0	29	1185	STCA
BW	22.6	−32.4	252.2	3.0	30	849	STCSA
MM	18.7	−33.5	638.1	6.0	32	203	
HM	19.3	−34.4	700.5	8.0	28	27	STCSH
CR	19.3	−33.4	716.3	6.0	31	457	
BD	20.1	−34.5	446.2	7.0	25	84	
LG	21.9	−32.8	133.1	3.0	32	555	STWA
LS	21.3	−33.5	364.7	5.0	31	544	
CW	18.9	−32.2	310.1	8.0	33	96	
PK	18.8	−32.9	388.1	6.0	32	203	
SW	20.4	−34.0	509.9	7.0	29	128	STWSA
SB	21.4	−34.4	435.1	7.0	26	36	
OD	22.2	−33.6	470.9	6.0	28	319	
MB	19.7	−33.4	311	4.0	29	2249	STWSH
PA	22.0	−33.2	354.3	4.0	29	633	

MG Murraysburg, BW Beaufort West, *MM* Malmesbury, *HM* Hermanus, *CR* Ceres, *BD* Bredasdorp, *LG* Leew Gamka, *LS* Ladismith, *SB* Still Bay, *OD* Oudtshoorn, *SW* Swellendam, *PK* Piketberg, *MB* Matroosberg, *CW* Clan William, *MB* Matroosberg, *PA* Prince Albert

0.11° in latitude and longitude (12.5 km × 12.5 km). Since historical data had missing values and there was large distances between gauging stations reanalysis data played a key part in solving these challenges (Gidey et al. 2018). Additional precipitation data were also obtained from the South Africa Weather Service from the period 1980–2020. These datasets were employed as a standard for forecasting the likelihood of drought occurrence in the study area.

Data processing and analysis

There exists uncertainty in analysing coarse resolution GCM outputs to catchment based finer scale resolution. As such there is a requirement to downscale GCM output for practical needs such as precipitation projection for hydrologic operations in local basins under climate change. Downscaling of MIROC6 output was conducted to provide finer resolution precipitation datasets and evaluate the output with reanalysis data. The software package Climate Change for Water Modeling (CMhyd) software obtained from https://swat.tamu.edu/software/cmhyd was used for bias correction and statistical downscaling. Before processing and analysis was performed on the historical, reanalysis data and downscaled climatic data, it was crucial to verify homogeneity and to perform data quality checks. To verify the homogeneity of climatic data, gross error checking, and temporal and spatial coherency tests were carried out. The accuracy of MIROC6 simulation to predict future precipitation data was evaluated using historical datasets to ensure their suitability before they were applied for calculating SPI indices. The percentage accuracy of the projected precipitation data was validated by comparing simulated reanalysis MIROC6 climate model data with historical CRU TS Version 4.07 precipitation data for the years 1980–2010. Results were evaluated in terms of mean absolute error (MAE), coefficient of determination (R^2), mean absolute percent error (MAPE) using the Eqs. (1–4) shown below:

$$MAD = \frac{1}{n}\sum_{1}^{n}(A_i - F_i) \tag{1}$$

$$MAPE = \frac{1}{n}\sum_{1}^{n}\left(\frac{(A_i - F_i)}{A_i} * 100\right) \tag{2}$$

$$R^2 = \frac{\sum_1^n (A_i - \overline{F_i})(F_i - \overline{F_i})}{\sum_1^n \left[\left(A_i - \overline{F_i}\right)^2\right)^{0.5}\left[\left(F_i - \overline{F_i}\right)^2\right)^{0.5}} \tag{3}$$

$$NSE = 1 - \left(\frac{\sum_1^n (A_i - F_i)^2}{\sum_1^n ((A_i - \overline{F_i})^2)}\right) \tag{4}$$

where A_i is the observed precipitation at timescale i, F_i is the projected precipitation at timescale i, $\overline{F_i}$ is the mean projected precipitation during the study period, and n is the total number of the observed data. The NSE illustrates

the percentage accuracy of the modeled data. Both R^2 and MAPE are measures of best line of fit, while MAD illustrates the global climate model's ability to correctly predict the future climate with respect to recorded data. It is assumed that the GCM simulation are correct when R^2 and NSE evaluations are close to unit value, and when there is a lower MAPE value (Das et al. 2019). A detailed explanation of techniques applied in the data analysis of the simulated precipitation data is in the sections below.

Precipitation variability

Variability in precipitation data is represented by regular fluctuations that take place at several repeated frequencies (Das et al. 2019). The variability component in precipitation data has a direct effect on the onset, duration and cessation of rainfall which affects the spatial and temporal characteristics of droughts (Gidey et al. 2018a). As such before assessing the characteristics of meteorological drought trends it was critical to assess the annual variability of precipitation data. Assessing both the yearly and seasonal rainfall variability across the agroecological zones in the present study provided good insight on how to deal with the frequency of droughts. Precipitation variability was assessed through the determination of coefficient of variability using the formula given by Eq. (5).

$$\%\ Coefficient\ of\ Variation\ (CV) = \frac{\sigma}{\dot{x}} * 100 \tag{5}$$

where σ = standard deviation and $\dot{x}$ = average rainfall between 1991 and 2020.

Trend analysis

A trend is the embedded and established monotonic element in climate data that may be a shifting pattern across the study period (Ndebele et al. 2020). Different techniques are employed to analyze trends in climate data, and these include slope-based tests such as the squares linear regression methods and Theil Sen's slope (Sonali and Nagesh Kumar 2013) and rank-based tests such as the Mann–Kendall (M–K) test (Mann 1945); and Spearman rank correlation (Das et al. 2019). The use of the Mann–Kendall test is widely recommended by the WMO, mainly because climate time series data does not necessarily follow a normal distribution. The Mann–Kendall test also has little sensitivity to sudden incoherence and breaks in data (Alhaji et al. 2018). As such the Mann–Kendall test was used to precipitation and SPI data points x_i that were ranked from $i = 1, 2 \ldots n-1$ and x_j, which were ranked from $j = i+1, 2 \ldots n$. All data points x_i were taken as a reference point and assessed against all the data points (Eq. 3–6) x_j, so that:

$$\mathrm{sgn}(x_j - x_i) = \begin{cases} +1, & if\ (x_j - x_i) > 0 \\ 0, & if\ (x_j - x_i) = 0 \\ -1, & if\ (x_j - x_i) < 0 \end{cases} \tag{6}$$

The M–K test parameter was calculated by:

$$S = \sum_{t=1}^{n-1} \sum_{j=i+1}^{n} \mathrm{sgn}(x_j - x_i) \tag{7}$$

The variation parameter was calculated by:

$$\mathrm{Var}(S) = \frac{1}{18}\left[n(n-1)(2n+5) - \sum_{i=1n}^{n-1} t_i(t_i - 1)(2t_i + 5)\right] \tag{8}$$

where t_i is the measure of ties in the data series i. The test statistic was calculated by:

$$Z_s = \begin{cases} \frac{S-1}{\sqrt{(\mathrm{Var}(S))}}, & if\ S > 0 \\ 0, & if\ S = 0 \\ \frac{S+1}{\sqrt{(\mathrm{Var}(S))}}, & if\ S < 0 \end{cases} \tag{9}$$

where $Z_s > 0$ signifies a rising trend, whereas $Z_s < 0$ signifies declining trend. Trend analyses are carried out at the particular significance level, α. In the present study, $\alpha = 0.05$ was employed. At, $\alpha = 0.05$, the null hypothesis of no trend was excluded if $|Z_s| > 1.96$ (Mann 1945).

Standardized Precipitation Index (SPI)

The SPI drought index is widely regarded by the WMO as a universal drought index (McKee et al. 1993). It is capable of assessing the characteristics of both dry and wet environments and its computation demands only historical precipitation records. On different time scales, the SPI provides a good overview of water excess or moisture deficiency in the soil (Basak et al. 2022). Since long-term precipitation data does not follow a normal distribution curve and as such requires adjusting it to a standard normal distribution. The SPI values are derived across 1-, 3-, 6-, 12-, 18-, and 24-month timescale. The SPI-1 has the capability to depict soil moisture and crop stress levels, SPI-3 depicts short term and medium-term moisture condition; SPI-6 represents changes in streamflow and reservoir level, SPI-9 depicts the precipitation patterns over a medium scale while the SPI-12 is useful for changes in surface runoff and groundwater levels (Mishra and Nagarajan 2011). Svoboda et al. (2012) recommended the use of 1-, 3- and 6-month timescales to characterize meteorological and agricultural droughts, and an SPI-12 or more for assessing changes in surfaces runoff (Nam et al. 2017). In the same vein, Vishwakarma et al. (2020) agrees with Svoboda et al. (2012) and recommends

that use of SPI index value at 3-, 6- and 12-month timescales is appropriate for depicting changes to precipitation patterns over a medium scale and streamflow, reservoir levels and even ground water levels at longer time scale in any catchment. The derivation of SPI values across 1-, 3-, 6-, 12-, 18-, and 24-month timescale involves using a Gamma Probability distribution function to derive the relative frequency distribution of observed averaged rainfall across the chosen time scale. The Gamma Probability Distribution function then transforms raw precipitation data into a standardized normal distribution function (Buttafuoco et al. 2018). The SPI index values were then attained by changing the cumulative probability of precipitation data into the standardized normal distribution using Eqs. (10)–(12) below:

$$g(x) = \frac{1}{((\beta^{\alpha})(\Gamma(\alpha))} x^{(\alpha-1)} e^{-\frac{x}{\beta}} \quad \text{for } x > 0 \tag{10}$$

where α = shape parameter, β = scale factor, x = amount of rainfall and Γ(α) = gamma function. The SPI was then calculated using the cumulative probability function as follows:

$$G(x) = \int_0^x g(x)dx = \frac{1}{((\beta^{\alpha})(\Gamma(\alpha))} \int_0^x x^{(\alpha-1)} e^{-\frac{x}{\beta}} dx \tag{11}$$

where G(x)= cumulative probability of the observed rainfall. The Gamma function is indefinite for x = 0. In this study, the cumulative probability function was analyzed as follows:

$$F(x) = p + (1 - p)G(x). \tag{12}$$

where p = probability of zero.

Therefore, to determine future drought events, the SPI developed was applied in analyzing projected precipitation datasets generated using the MIROC6 model under the SSP5–8.5, SSP2–4.5 and SSP1–2.6 climate change scenarios. The temporal features of meteorological drought were assessed through the derivation of SPI value, calculated at 12-month timescale using R. The calculated SPI values typically range from − 2.00 (very dry) to + 2.00 (wet). A SPI < 0 value indicated periods of drought stress, while a SPI > 0 indicated wet conditions. Depending on the magnitude of the SPI index value, the degree of severity of the drought was determined according to the classification criteria shown in Table 2.

Table 2 Standardised Precipitation Index (SPI) (McKee et al. 1993)

SPI interval	Classification	Acronym
0 < SPI ≤ 2	Above normal condition	ANC
− 1 < SPI ≤ 0	Mild drought	MiD
− 1.5 < SPI ≤ − 1	Moderate drought	MoD
− 2 < SPI ≤ − 1.5	Severe drought	SD
SPI ≤ − 2.0	Extreme drought	ED

Analysis of drought duration, magnitude, intensity, and frequency

Analysing the drought magnitude, intensity and frequency requires stochastic approaches, however to date no standard methodology exists has been proposed to accurately determine drought duration. (Sirdas and Sen 2003). Once drought magnitude, intensity and frequency are objectively determined, it is achievable to effectively manage future drought risk in vulnerable areas. Drought magnitude, intensity and frequency was quantitatively analyzed based on SPI-12 values. However, in this study drought duration was articulated as the number of consecutive drought days or periods. The length of the drought episode (m) was defined as equal to the number of years between drought onset (i) and end year (e). The drought duration was determined based on the number of successive drought events. The magnitude of future drought episodes was calculated using Eq. (13) as follows:

$$M = \sum_{i=1}^{m} (Drought\ Index)_i \tag{13}$$

where M = drought magnitude, m = drought months, Drought Index = SPI value in ith time scale.

Mishra and Nagarajan (2011) defined drought intensity as the ratio of the drought magnitude to its duration. The intensity of future drought in the near term (2021–2050) was calculated using Eq. (14) as follows:

$$I_e = \frac{M}{m} \tag{14}$$

where I_e = intensity, M = drought magnitude, m = drought duration.

The drought frequency occurrence was related to other aspects, such as drought magnitude and intensity. The frequency of drought was calculated using Eq. (15) as follows:

$$F_e = \frac{n_s}{N_s} * 100 \tag{15}$$

where n_s is the total drought events and N_s is number of years for the study period, which in this research study was 30 years.

Results

Validation

Table 3 lists the evaluation metrics that were used when validating the simulated precipitation datasets; the mean

Table 3 Validation metrics of projected precipitation

Station	Mean absolute deviation (MAD) (mm)	Coefficient of determination (R^2)	Mean absolute percent error (MAPE)	NSE model	AEZ
MG	59.6	0.87	19.18	80.83	STCA
BW	39.7	0.83	15.75	84.25	STCSA
MM	108.3	0.86	16.97	83.03	STCSH
HM	134.3	0.87	19.18	80.83	
CR	116.1	0.88	16.22	83.79	
BD	124.0	0.88	16.58	83.42	
LG	22.6	0.87	16.97	83.03	STWA
LS	71.1	0.86	19.49	80.51	
CW	51.4	0.88	16.56	83.44	STWSA
PK	62.9	0.86	16.22	83.79	
SW	99.4	0.87	19.50	80.50	
SB	84.8	0.89	19.49	80.51	
OD	94.1	0.87	19.99	80.01	
MB	111.8	0.87	16.66	83.34	STWSH
PA	132.1	0.86	21.50	78.50	

MG Murraysburg, *BW* Beaufort West, *MM* Malmesbury, *HM* Hermanus, *CR* Ceres, *BD* Bredasdorp, *LG* Leew Gamka, *LS* Ladismith, *SB* Still Bay, *OD* Oudtshoorn, *SW* Swellendam, *PK* Piketberg, *MB* Matroosberg, *CW* Clan William, *MB* Matroosberg, *PA* Prince Albert

absolute deviation (MAD), coefficient of determination (R^2), mean absolute percent error (MAPE) and Nash–Sutcliffe efficiency (NSE) model. The results of validation metrics of near-term precipitation data (2021–2050) with the reanalysis precipitation data (1991–2010) in the agroecological zones of the study area gave a good insight on the accuracy of the projected precipitation data with the observed data (Table 3). The results indicate that the lowest MAD of 22.6 mm was observed in Leew Gamka located in the STCSA, while the highest MAD was observed in Hermanus at 134.3 mm. Stations in the sub-humid zones had higher MAD values compared to stations in the arid zones. Results from Table 3 illustrate that MAPE values ranged from 15.8% in Beaufort West located in the STCSA to 21.50% in Prince Albert found in STWSH. The coefficient of determination results indicates a minimum value 0.83 at Beaufort West located in STCSA while 0.89 was recorded in STWSA (Still Bay) (Table 3). The NSE model of the projected precipitation measured in the study period (2021–2050) was illustrated to be greater than seventy percent (70%), with greatest value recorded at Beaufort West while Prince Albert recorded the lowest value at 78.5% (Table 3).

Annual precipitation trends

Table 4 illustrates the calculated values of the MAP, CV, and precipitation trends between 2021 and 2050 under the SSP5–8.5, SSP2–4.5, and SSP1–2.6 climate change scenarios. The results of long-term annual precipitation variability in the agroecological zones of Western Cape Province provided a good understanding on how to cope with recurrent droughts. The results from Table 4 reveal that under the SSP5–8.5 climate scenario the mean annual precipitation is predicted to be between 98 mm in Leew Gamka in STCSA and 314 mm in Malmesbury found in STCSH. The results from Table 4 reveal that under the SSP2–4.5 climate scenario the mean annual precipitation is predicted to be between 250 mm in Beaufort West in STWA and 252 mm in Murraysburg found in STCA. The results from Table 4 also reveal that under the SSP1–2.6 climate scenario the mean annual precipitation is predicted to be between 224 mm in Leew Gamka in STWA and 311 mm in Murraysburg found in STCA Table 4. Overall, the results indicate that STCSA recorded the lowest mean annual precipitation under the three climate change scenarios (Table 4).

The results from Table 4 reveal that under the SSP5–8.5 climate scenario the coefficient of variability is predicted to be between 58% in Swellendam in STWSA and 32% in Hermanus found in STCSH. The results from Table 4 reveal that under the SSP2–4.5 climate scenario the coefficient of variability is predicted to be between 35% in Murraysburg in STCA and 48% in Bredasdorp found in STCSH. The results from Table 4 reveal that under the SSP1–2.6 climate scenario the coefficient of variability is predicted to be between 40% in Ceres in STCSH and 47% in Hermanus found in STCSH. Overall, the results from Table 4 indicate that Leew Gamka recorded the lowest mean annual precipitation under the three climate change scenarios. The results illustrate that under the SSP5–8.5 the precipitation trends across all AEZs were predicted to be statistically significant negative trends (Table 4). Maximum statistically negative trends of − 7.6 mm/year were recorded at Ceres in STCSH while

Table 4 Changes in projected precipitation

Station	Mean annual precipitation (mm)			Coefficient of variation (% CV)				Trends (Sig.) (mm/year)			AAEZ
	SSP5–8.5	SSP2–4.5	SSP1–2.6	SSP5–8.5	SSP2–4.5	SSP1–2.6	Obs	SSP5–8.5	SSP2–4.5	SSP1–2.6	
MG	252	261	311	42	35	42	− 1.0 (− 1.2)	**− 3.5 (− 2.1)**	**− 1.7 (− 2.0)**	− 0.4 (0.0)	STCA
BW	110	250	226	45	36	42	− 1.0 (− 1.2)	**− 2.9 (− 2.0)**	− 1.2 (− 1.1)	− 0.1 (1.0)	STCSA
MM	98	314	254	40	37	43	**− 6.4 (− 2.7)**	**− 5.9 (− 2.1)**	1.9 (− 0.7)	0.3 (1.1)	STCSH
HM	120	303	277	32	40	47	**− 6.5 (− 2.7)**	**− 6.6 (− 2.2)**	**− 1.5 (− 2.1)**	− 0.1 (0.3)	
CR	111	283	234	39	48	40	**− 7.8 (− 2.7)**	**− 7.6 (− 2.5)**	− 1.1 (− 2.1)	− 0.3 (0.1)	
BD	107	300	268	56	48	46	**− 4.1 (− 2.3)**	**− 5.2 (− 2.1)**	− 0.8 (− 0.4)	0.1 (0.1)	
LG	120	250	224	53	37	45	**− 4.2 (− 2.3)**	**− 4.8 (− 2.2)**	0.3 (− 0.7)	− 0.3 (− 0.1)	STWA
LS	98	277	245	43	37	44	**− 4.2 (− 2.3)**	**− 4.9 (− 2.1)**	**− 1.2 (− 2.1)**	0.2 (0.1)	
CW	109	281	235	46	37	45	**− 2.4 (− 2.4)**	**− 3.8 (− 2.0)**	− 0.2 (0.0)	0.2 (0.0)	STWSA
PK	105	291	240	56	38	45	**− 3.6 (− 2.6)**	**− 3.7 (− 2.2)**	− 1.3 (− 1.2)	0.1 (0.1)	
SW	110	266	227	58	39	46	**− 5.2 (− 2.4)**	**− 5.4 (− 2.1)**	**− 1.4 (− 2.2)**	− 0.3 (− 0.1)	
SB	104	300	268	43	37	46	− 3.9 (− 1.7)	**− 4.2 (1.9)**	− 0.6 (− 0.1)	0.2 (− 0.1)	
OD	120	276	246	41	37	45	**− 4.4 (− 1.9)**	**− 4.0 (− 2.3)**	− 0.2 (0.2)	− 0.1 (− 0.1)	
MB	109	283	235	43	37	44	**− 3.2 (− 2.8)**	**− 4.6 (3.1)**	− 0.2 (− 0.2)	− 1.2 (0.1)	STWSH
PA	107	257	228	46	38	46	**− 3.4 (− 3.0)**	**− 4.6 (− 2.7)**	**− 2.2 (− 2.1)**	0.0 (0.1)	

MG Murraysburg, *BW* Beaufort West, *MM* Malmesbury, *HM* Hermanus, *CR* Ceres, *BD* Bredasdorp, *LG* Leew Gamka, *LS* Ladismith, *SB* Still Bay, *OD* Oudtshoorn, *SW* Swellendam, *PK* Piketberg, *MB* Matroosberg, *CW* Clan William, *MB* Matroosberg, *PA* Prince Albert

Bold face in the table reflects statistically significant trends

minimum values of − 2.9 mm/year were observed in Beaufort West in STCSA (Table 4). These findings from Table 4 indicate a steady improvement from − 7.8 mm/year under the observation period 1980–2020 and a worsening trend in Beaufort West in STCSA from − 1.0 mm/year also under the observational period (1980–2020). The results from Table 4 illustrate that under the SSP2–4.5 climate change scenario the precipitation trends were predicted to be both negative and positive trends across the AEZs (Table 4). Maximum statistically significant negative trends of − 2.2 mm/year were observed at Prince Albert in STWSH while statistically insignificant trends of 1.9 mm/year were observed in Malmesbury in STCSH. These findings from Table 4 indicate a progressive improvement from − 3.4 and − 6.4 mm/year in the same regions respectively under the historical trends observed between 1980 and 2020 (Table 4). Under the SSP1–2.6 scenario the result indicate that the precipitation trends were predicted to be both negative and positive trends (Table 4). Maximum statistically insignificant negative trends of − 1.2 mm/year were recorded at Matroosberg in STWSH while maximum positive trends of 0.3 mm/year were observed in Still Bay in STWSA and Malmesbury in STCSH (Table 3). Overall, the findings from Table 4 indicate a progressive improvement across the climate change scenarios with SSP5–8.5 indicating statistically significantly negative trends while both the SSP2–4.5 and SSP1–2.6 indicated mostly positive insignificant precipitation trends in the near term (2021–2050).

Future meteorological droughts prediction based on SPI-12

The results of drought prediction where based on Figs. 2, 3 and 4 illustrate the temporal variation of future meteorological drought events derived through the SPI-12 across all the AEZs. Values of SPI < 0 across the study area indicated drought periods at various severity levels, while SPI > 0 indicated wet periods according to the McKee et al. (1993) categorization method. The results were analysed across each climate scenario for each AEZ.

Drought prediction based on SSP5-8.5

In the STWSA zone under the SSP5-8.5 climate scenario, the results suggest that throughout the study period drought episodes were predicted, in Oudtshoorn with the most severe drought occurring in 2021, 2025–2028 and 2041 (Fig. 2). The results indicate that Piketberg is anticipated to observe longer duration droughts in the years 2029 to 2033; 2037, 2040, 2042 and 2047 being the only years were normal to above normal conditions were experienced (Fig. 2). Clan William and Still Bay were predicted to experience less drought incidences compared to other station in STWSA, with Still Bay projected to experience mild drought only four times across the study period (Fig. 2). In the STCSH zone, the results indicate that Ceres experienced sustained drought periods throughout the study period, with the most extreme drought incident taking place in 2022 and 2044 (Fig. 3). Similarly, Hermanus is projected to suffer from longer drought periods, starting off as mild drought in the years 2026 to 2038, 2039 to 2040 and 2045 to 2050, while the years 2024 and 2025 are projected to be wet (Fig. 3). Malmesbury and Bredasdorp largely experienced wet conditions during the study period with Malmesbury only experiencing mild drought conditions in 2024, 2039 and 2042, while Bredasdorp is anticipated to observe moderate drought in 2025 (Fig. 3). In the STCSA the results indicate that Beaufort West will observe drought thought the study period (Fig. 3). The results indicate that in the STCA, Murraysburg experienced predominantly normal to wet conditions, while during the years 2025, 2027, 2038, 2042, 2044 there was mild drought (Fig. 4). In STWA the results project predominantly drought conditions in Ladismith with only the years 2025–2026, 2037, 2042 and 2042–2045 predicted to be wet (Fig. 4). In STWSH, sustained drought periods are expected in Murraysburg while in Prince Albert, multi-year drought periods are projected particularly between 2027 and 2037 (Fig. 4).

Drought prediction based on SSP2-4.5

In the STWSA zone under the SSP2-4.5 climate scenario, the findings indicate that throughout the study period drought episodes were projected in Oudtshoorn with the most severe drought occurring in 2041 as well as in 2045 (Fig. 2). The findings from Fig. 2 indicate that next region to be severely affected by drought is Piketberg. The results indicate that Piketberg will also undergo severe in 2043, while Clan William and Still Bay were projected to experience predominantly wet conditions (Fig. 2). The results indicate that Still Bay will have droughts only during the years 2034, 2040–2041 and 2046. In the STCSH, the results indicate that Ceres experienced sustained drought periods with wet conditions in 2030–2031, 2041, 2043 and 2050 (Fig. 2). Hermanus is projected to experience more frequent drought conditions, however the drought episodes appear to be less compared to the ones anticipated under the SSP5-8.5 climate scenario (Fig. 3). Malmesbury is also expected to experience largely wet conditions similar to the results obtained under climate scenario SSP5-8.5 (Fig. 3). Bredasdorp experienced more drought events compared to the SSP5-8.5 climate scenario. In the STCSA zone the results indicate that Beaufort West will observe drought thought the study period (Fig. 3). In the STCA, Murraysburg experienced predominantly normal to wet conditions, particularly between the years 2021–2028, 2033–2037 2045 to 2047

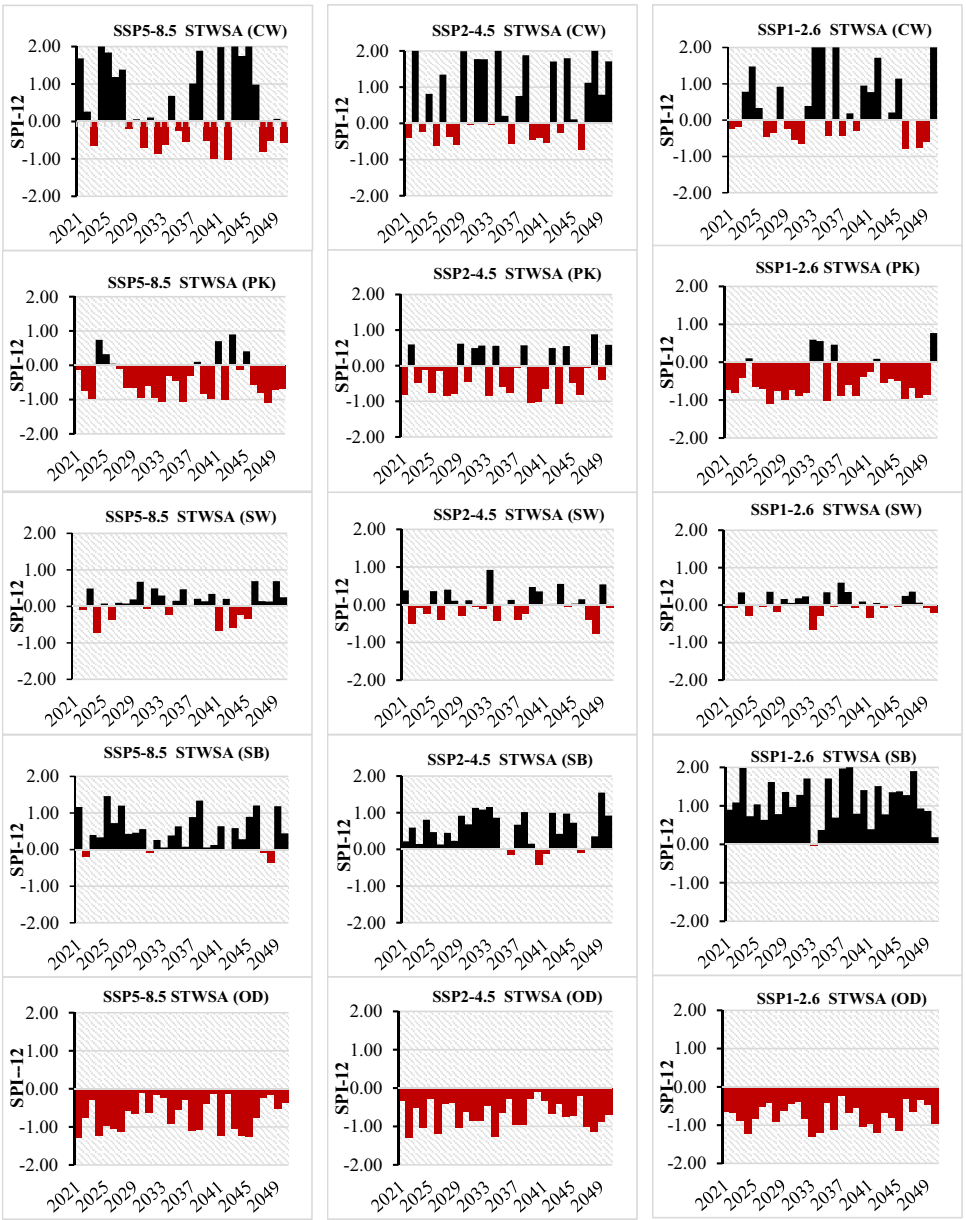

Fig. 2 Temporal variation of future meteorological drought events

(Fig. 4). In STWA the results project predominantly wet conditions in Ladismith with moderate drought conditions expected in 2025, 2040 and 2042 (Fig. 4). In STWSH zone sustained drought periods are expected in Matroosberg, with only wet conditions expected in 2028, 2040–2041 and 2046 while in Prince Albert, there is going to be more frequent drought periods with a mild drought after every two years (Fig. 4).

Drought prediction based on SSP1-2.6

In the STWSA zone under the SSP1-2.6 climate scenario the results suggest that throughout the study period drought episodes were predicted, in Oudtshoorn with the most severe drought occurring between 2033 and 2034 (Fig. 2). The results indicate that Piketberg is anticipated to observe longer duration droughts the years 2024 to 2032; 2037 to 2041 and between 2042 and 2049 (Fig. 2). The years 2024, 2033–2034, 2037 and 2050 are anticipated to be wet years in Piketberg (Fig. 2). In Clan William it is predicted that less severe drought incidences, will take place compared to climate scenarios SSP5–8.5 and SSP2–4.5 (Fig. 2). Still Bay is projected to experience wet conditions across the study period (Fig. 2). In the STCSH zone, the results indicate that Ceres experienced sustained severe drought periods throughout the study period (Fig. 3). Similarly, Hermanus is predicted to suffer from longer drought periods starting from the year 2021 to 2033, 2036 to 2042 and 2044 to 2049

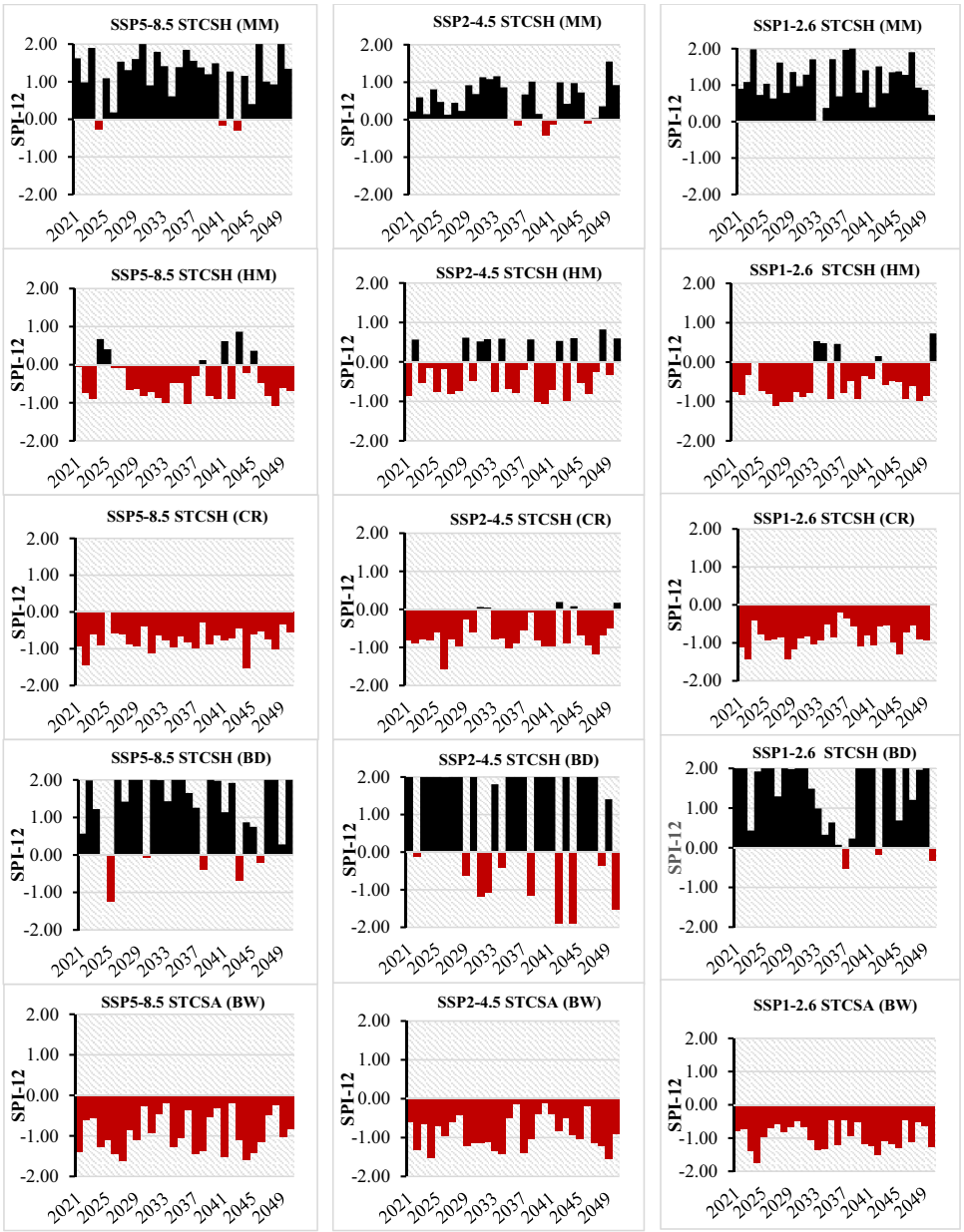

Fig. 3 Temporal variation of future meteorological drought events

while the years 2034 to 2035, 2037 and 2050 are years that are expected to be wet (Fig. 3). Malmesbury and Bredasdorp largely experienced wet condition during the study period with Bredasdorp only recording mild drought conditions in 2036, 2042 and 2050 (Fig. 3). In the STCSA the results indicate that Beaufort West will observe drought thought the study period (Fig. 3). The results indicate that in the STCA zone, Murraysburg experienced predominantly wet conditions, particularly between the years 2021 to 2033and 2045–2049, while in the years 2034, 2036, 2040 and 2050 severe drought conditions were anticipated (Fig. 4). In the STWA zone the results project predominantly wet conditions in Ladismith with 8 drought incidences throughout the 30 year study period, while Leew Gamka is expected to undergo mild to severe drought conditions with the year 2032–2033, 2036 and 2050 expected to be wet years (Fig. 4). In the STWSH zone sustained drought periods are expected in Matroosberg while in Prince Albert, multi-year drought periods are projected particularly between 2025 and 2032 and 2045 to 2048 (Fig. 4).

Future drought magnitude, intensity, and frequency

Table 5 gives the findings of the magnitude (M), intensity (I) and frequency (F) of the meteorological drought calculated over the study period (2021–2050). The magnitude, intensity and frequency of future drought calculated using the SPI-12 based on projected values of precipitation

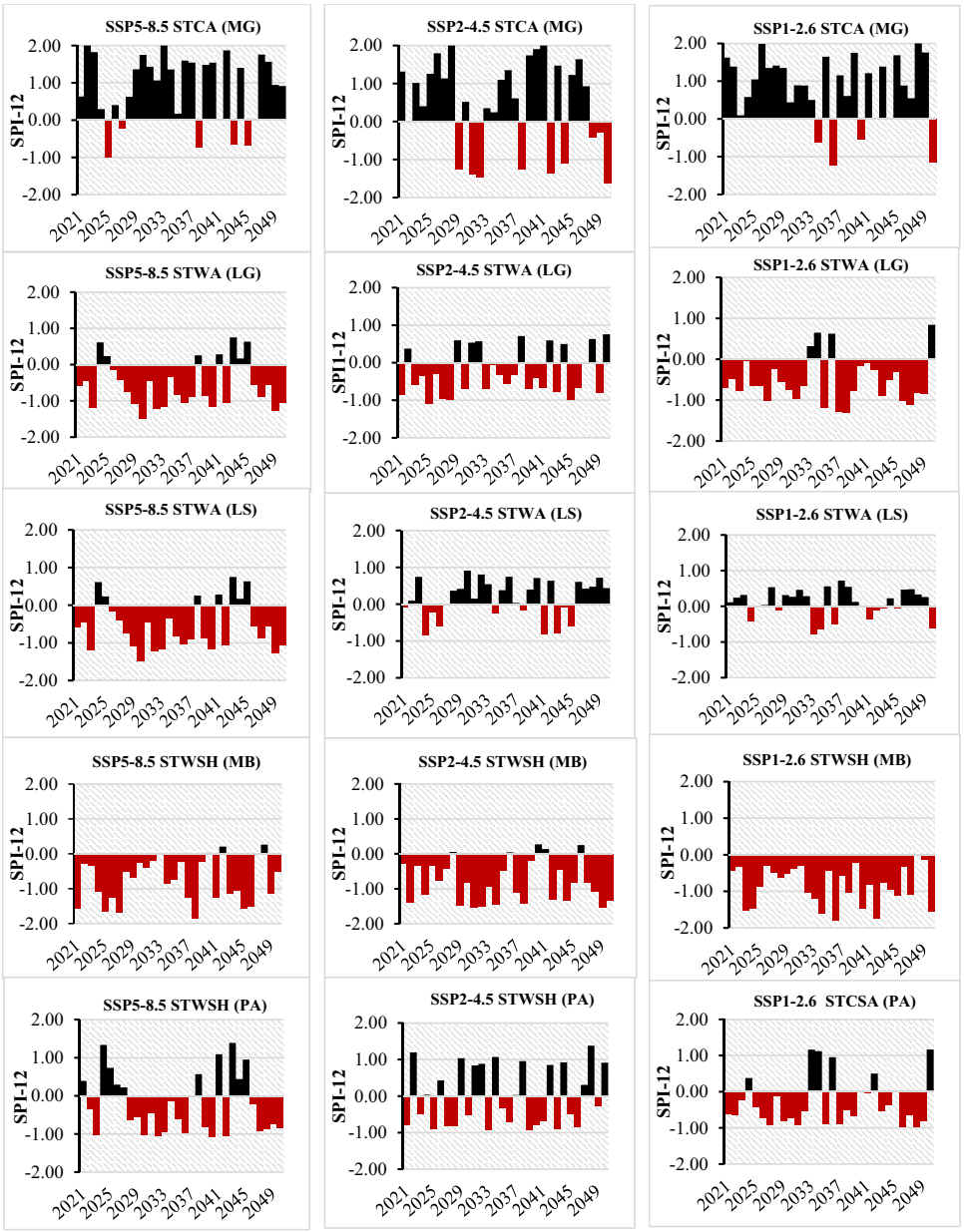

Fig. 4 Temporal variation of future meteorological drought events

from MIROC6 was particularly crucial in the assessment of projected water availability in streams in the various AEZs. The results from Table 5 illustrate that in areas around STCA maximum drought magnitude and frequency of 10.1 mm and 1 mm/year were predicted under the SSP2–4.5 climate change scenario while the greatest drought frequency was also predicted to be 33% (Table 5). The results indicate that in STCSA the SSP1–2.6 was the worst with a drought magnitude of 28.5 mm while the drought intensity and frequency were expected to be maximum at 1.0 mm/year and 100% respectively (Table 5). In the STCSH regions, Ceres district was predicted to have the greatest drought magnitude and intensity of 24.6 mm and 0.85 mm/year under the SSP1–2.6 climate change scenario while the greatest drought frequency was expected under the SSP2–4.5 climate change scenario at 100% (Table 5). The results from Table 5 illustrate that in the STWA regions the greatest drought magnitude was predicted to be in Leew Gamka at 19.6 mm, with a maximum intensity of 0.9 mm/year under the SSP5–8.5 climate scenario while the greatest frequency was expected in under the SSP1–2.6 climate scenario. The results indicated that under STWSA regions Oudtshoorn recorded the greatest drought magnitude of 22.4 mm under the SSP1–2.6 climate scenario with a frequency of 100% (Table 5). The drought intensity was expected to be greatest in Piketberg under the SSP5–8.5 climate scenario. Meanwhile in the STWSH regions Matroosberg had the greatest drought

magnitude, intensity, and frequency at 24.9 mm, 1.0 mm/year and 100% respectively (Table 5). Overall, the results indicate that across all the AEZs of the Western Cape, the most severe drought and ultimately greatest water availability challenges were predicted in Beaufort West under the SSP1–2.6 climate scenario with a drought magnitude of 28.5 mm while the drought intensity and frequency were expected to be 1.0 mm/year and 100% respectively (Table 5).

Drought ranking

Tables 6 and 7 present the characteristics of five high-ranked droughts in the AEZs based on maximum drought magnitude (M_{max}) and maximum drought intensity (I_{max})

Table 5 Predicted drought magnitude, intensity, and frequency

Station	SSP5–8.5			SSP2–4.5			SSP1–2.6			AEZ
	M (mm)	I	F (%)	M (mm)	I (mm)	F (%)	M (mm)	I (mm)	F (%)	
MG	3.33	0.7	20	10.1	1.0	33	3.6	0.7	17	STCA
BW	27.5	0.9	100	26.6	0.9	100	28.5	1.0	100	STCSA
MM	0.8	0.3	10	0.8	0.2	0.2	0.0	0.0	0	STCSH
HM	15.5	0.6	80	12.6	0.6	67	17.7	0.7	80	
CR	22.4	0.7	100	19.6	0.8	83.3	24.6	1.0	97	
BD	2.5	0.5	17	10.2	1.0	30	1.0	0.3	10	
LG	19.6	0.9	77	12.9	0.6	70	17.9	0.7	87	STWA
LS	4.4	0.4	37	6.7	0.5	46	3.7	0.3	43	
CW	8.3	0.6	46	5.3	0.4	46	5.8	0.4	47	STWSA
PK	15.6	0.8	77	12.2	0.6	0.7	17.4	0.7	80	
SW	3.3	0.3	40	4.1	0.3	50	2.9	0.2	50	
SB	0.7	0.2	16	0.8	0.2	17	0.0	0.0	0.0	
OD	20.4	0.7	100	20.4	0.1	100	22.4	0.7	100	
MB	23.2	0.9	86	24.2	0.9	83	24.9	1.0	100	STWSH
PA	14.4	0.7	70	11.2	0.7	53	14.2	0.6	80	

MG Murraysburg, BW Beaufort West, *MM* Malmesbury, *HM* Hermanus, *CR* Ceres, *BD* Bredasdorp, *LG* Leew Gamka, *LS* Ladismith, *SB* Still Bay, *OD* Oudtshoorn, *SW* Swellendam, *PK* Piketberg, *MB* Matroosberg, *CW* Clan William, *MB* Matroosberg, *PA* Prince Albert

Table 6 Drought ranking by magnitude

Ranking	Magnitude (mm)	AEZ (Station)	Scenario	Most extreme drought period Between 2021 and 2050		
				Start date	End date	Duration (days)
1	28.5	STCSA (BW)	SSP1–2.6	11 August 2023	22 March 2025	620
2	27.5	STCSA (BW)	SSP5–8.5	15 June 2044	30 August 2045	441
2	26.6	STCSA (BW)	SSP2–4.5	21 April 2026	13 May 2027	387
4	24.9	STWSH (MB)	SSP1–2.6	03 July 2036	10 April 2037	281
5	24.6	STCSH (CR)	SSP1–2.6	29 June 2028	11 May 2029	317

Table 7 Drought ranking by intensity

Ranking	Intensity (mm/year)	AEZ (Station)	Scenario	Most intense drought period Between 2021 and 2050		
				Start date	End date	Duration
1	1.0	STCSA (BW)	SSP1–2.6	11 August 2023	22 March 2025	620
2	1.0	STCSH (BD)	SSP2–4.5	21 April 2030	13 May 2031	388
3	1.0	STCSH (CR)	SSP1–2.6	29 June 2028	11 May 2029	317
4	1.0	STWSH (MB)	SSP1–2.6	03 July 2036	10 April 2037	281
5	1.0	STCA (MG)	SSP2–4.5	17 September 2039	30 June 2040	287

respectively across the study period (2021–2050). The results from Table 6 indicate that the top three greatest drought magnitudes will take place in the STCSA (BW). The results indicate that the greatest drought magnitude of 28.5 mm will occur under SSP1–2.6 climate change scenario. Similarly, in the STWSH and STCSH regions the fourth (24.9 mm) and fifth (24.6 mm) ranked drought magnitudes in Matroosberg and Ceres are occurring under the SSP1–2.6 climate scenario (Table 6). For drought events classified by their magnitude, there appears to be a logical positive correlation between the magnitude and frequency of drought for all events. The greatest future drought magnitude ($M_{max} = 28.6$ mm) is projected to elongate for as long as 620 days and the lowest magnitude future drought ($M_{min} = 24.6$ mm) in the top five ranked drought lasted only for 317 days as presented in (Table 6).

Meanwhile the results from Table 7 illustrated the characteristics of the top five drought events based on the intensity of the drought event calculated across the near 2021–2050 together with the duration of the most intense drought between 2021 and 2050. The results from Table 7 indicate that the top five ranked intense droughts are predicted to occur at 1.0 mm/year. Results from Table 7 indicate that 60% of these most intense drought events are expected to occur under the SSP1–2.6 climate scenario. The most affected regions are STCSH (BD and CR), STCA (MG), STWSH (MB) and STCSA (BW). The duration of the most intense drought event is expected to be 558 days in STCSA in Beaufort West while the least intense drought will have a duration of 638 days in STWSH (MB) (Table 7). Importantly Table 7 this event far exceeds the threshold of a severe drought for which the SPI-12 value is less than − 1.5.

Discussion

The overarching objective of this study was to assess the spatio-temporal characteristics of future meteorological drought in the near term (2021–2050) on the agroecological zones of the Western Cape Province in South Africa under the SSP5–8.5, SSP2–4.5 and SSP1–2.6 climate scenarios. The study sought to augment studies carried out by other scholars such as Orimoloye et al. (2019); Otto et al. (2018); Ziervogel (2019); Ziervogel et al. (2022) by examining the seasonality of the projected precipitation trends as well as understanding the perceptions of the communities on the future drought incidence. The drought magnitude, intensity frequency and drought ranking based on the magnitude and intensity was investigated in the near term (2021–2050) under the three climate change scenarios. The results of trend analysis of projected precipitation indicated a progressive improvement across the SSP5–8.5, SSP2–4.5 and SSP1–2.6 climate change scenarios. The results obtained under the SSP5–8.5 indicated statistically significantly negative trends while both the SSP2–4.5 and SSP1–2.6 indicated mostly positive insignificant precipitation trends in the near term (2021–2050). The negative trends in projected precipitation under the SSP5–8.5 indicated protracted drought across all the AEZs of the Western Cape Province. These results are in parity with those reported by Engelbrecht and Monteiro (2021), that suggested that not only will there be universal decreases in precipitation over southern Africa under the SSP5–8.5 climate change regime but recurrent droughts are also predicted to take place. Similarly, both negative and positive in SSP2–4.5 and SSP1–2.6 climate scenarios were expected to ease off the drought periods across the study period. These findings implied that in the near term, agricultural production in the agroecological zones was expected to substantially decline particularly in areas that relied mostly on rainfed agriculture. These findings were also in agreement with studies by Thomson et al. (2011) who reported on the RCP4.5 as a stabilization pathway to climate change. The study noted that the probable source of negative trends in precipitation could be climate change and anthropogenic activities such as increased population growth and urbanisation as suggested by scholars such as Park et al. (2015) who have under taken similar studies in Korea.

Based on the SPI-12 results regions in STWSH (MB), STCSA (BW) and STWSA (OD) were predicted to have sustained drought period throughout the near term across the climate change scenarios. This implied that these AEZs were expected to have chronic water shortages as will be evidenced through reduced stream-flows. The greatest drought magnitude was predicted to happen in the STCSA (BW) under the SSP1–2.6 climate change scenario. This projection was almost similar with the projection suggested by Botai et al. (2017) who used historical observed station data and reported that in the near term the Western Cape was expected to experience more severe drought incidences unless strict climate change mitigation strategies were implemented. The AEZs that were found close to coastal regions of South Africa revealed mostly positive SPI values, although future drought episodes appeared to become milder, particularly in the western coast as a consequence of changes in land-use and land cover patterns. This finding was in contrast with other findings from previous studies by scholars such as Otto et al. (2018) and thus necessitates further focused investigation. Based on analysis of the results of the SPI-12 a maximum intensity of 0.5–1.0 mm/year was deducted for most agroecological zones. This finding concurred with the projected increase in drought intensity previously found by Orimoloye et al. (2019) using geospatial datasets. Another important outcome of this study was the numerical predictability of drought in the Western Cape using the SPI within the framework of global climate model (MIROC6) under the three climate change scenarios used in the present study. The

results from this study also indicated that community members within the agroecological zones were not fully aware of when future drought episodes will occur, and this affected their adaptive capacity to the impacts of projected frequent, severe, and intense drought events. These results were in parity with studies undertaken by Baudoin et al. (2017), which suggested that early warning signals were generally not reliable. Conclusively, future drought characterisation in the WC province of South Africa provided suitable reference information for judicious monitoring and prediction of drought incidence based on a suitable index (e.g., SPI-12) and household survey. A blend of drought evaluation indicators was useful to assess the relative impacts of drought in different AEZs of future drought incidence, support proactive agricultural planning to reduce the influences of recurrent drought on sustainable livelihoods.

Conclusion

Climate change and anthropogenic activities have considerably aggravated the prospects of sustained future drought incidence, however, there still remains little awareness on this phenomenon from communities in countries in the global south. This study serves as a prelude to possibilities of more detailed analyses to come. Although the best readily available regional projections of climate change were used here, it was admittedly an incomplete comparison. The drought prediction findings from this reveal that this trend will significantly affect water availability and consequently affect agricultural production in agro-ecological regions. Trend analysis results from previous research revealed a projected decline in precipitation received across all the climate change scenarios as well as in drought incidence across all AEZs. This motivated us to focus on precipitation as the single most important variable from which to predict the effects of human induced climate change on water availability and agricultural production in the Western Cape. The negative trend in annual precipitation revealed by the study in the agroe-cological zones means less available water for crops amplifying the gap between water supply and demand in crop production for farmers. The impact of drought in the agro-ecological zones will increase the water stress and consequently water related conflicts from farmers withdrawing water from the same reservoirs because of competition for the same resource. Conclusively, while the Western Cape Province averted 'Day Zero', at the cost of agricultural production the predicted drought incidence in this study, the dependence on domestic and agricultural water supply from rain-fed reservoirs coupled with population growth, provides a need to review the current water governance frameworks to adapt to changing risks. Possible solutions include expanding existing domestic water sources through desalination and groundwater abstraction along with nature-based solution that ensure natural groundwater recharge. Furthermore, this study proposes for more research that seeks to gain more insight on the role of not only precipitation but also temperature on future drought prediction and the associated impacts on water availability and agricultural production.

The limitations of the study were that that projections used were not wholly consistent with historical observed data and in terms of periods and boundary forcing. A more consistent set of projections was not available, which is a common state for climate science in the developing world. The most extensive sets of consistently produced climate projections currently existing have been made for Europe. However, an initiative is underway to provide an extensive quality-controlled dataset of future regional climate projections for other regions around the globe—the Coordinated Regional Climate Downscaling Experiment organised under the World Climate Research Programme (WCRP). Africa is a priority region within CORDEX. With a more extensive and consistent set of future climate projections, more detailed analyses can be performed for assessing impacts on hydrology and water resources, including improved methods to prioritise or weigh results within the ensemble of outcomes.

Funding Open access funding provided by University of the Witwatersrand.

Data availability Data will be made available on request.

Declarations

Conflict of interest No conflict of interest is embedded in the research paper.

References

Abiodun BJ, Makhanya N, Petja B, Abatan AA, Oguntunde PG (2019) Future projection of droughts over major river basins in Southern Africa at specific global warming levels. Theor Appl Climatol 137(3):1785–1799. https://doi.org/10.1007/s00704-018-2693-0

Alhaji UU, Yusuf AS, Edet CO, Oche CO, Agbo EP (2018) Trend analysis of temperature in Gombe State using Mann Kendall trend test. J Sci Res Rep. https://doi.org/10.9734/JSRR/2018/42029

Basak A, Rahman ATMS, Das J, Hosono T, Kisi O (2022) Drought forecasting using the Prophet model in a semi-arid climate region of western India. Hydrol Sci J 67(9):1397–1417. https://doi.org/10.1080/02626667.2022.2082876

Baudoin M-A, Vogel C, Nortje K, Naik M (2017) Living with drought in South Africa: lessons learnt from the recent El Niño drought period. Int J Disaster Risk Reduct 23:128–137. https://doi.org/10.1016/j.ijdrr.2017.05.005

Blamey RC, Middleton C, Lennard C, Reason CJC (2017) A climatology of potential severe convective environments across South Africa. Clim Dyn 49(5):2161–2178. https://doi.org/10.1007/s00382-016-3434-7

Botai CM, Botai JO, De Wit JP, Ncongwane KP, Adeola AM (2017) Drought characteristics over the Western Cape Province, South Africa. Water 9(11):Article 11. https://doi.org/10.3390/w9110876

Burke EJ, Brown SJ, Christidis N (2006) Modeling the recent evolution of global drought and projections for the twenty-first century with the Hadley Centre Climate Model. J Hydrometeorol 7(5):1113–1125. https://doi.org/10.1175/JHM544.1

Buttafuoco G, Caloiero T, Ricca N, Guagliardi I (2018) Assessment of drought and its uncertainty in a southern Italy area (Calabria region). Measurement 113:205–210. https://doi.org/10.1016/j.measurement.2017.08.007

Calverley CM, Walther SC (2022) Drought, water management, and social equity: analyzing Cape Town, South Africa's water crisis. Front Water. https://doi.org/10.3389/frwa.2022.910149

Christensen JH, Hewitson B, Busuioc A, Chen A, Gao X, Held I, Jones R, Kolli RK, Kwon WT, Laprise R, Magana Rueda V, Mearns L, Menendez CG, Raisanen J, Rinke A, Sarr A, Whetton P (2007) Regional climate projections. Chapter 11. https://www.osti.gov/etdeweb/biblio/20962141

Das J, Mandal T, Saha P (2019) Spatio-temporal trend and change point detection of winter temperature of North Bengal, India. Spatial Inf Res 27(4):411–424. https://doi.org/10.1007/s41324-019-00241-9

Dennis I, Dennis R (2012) Climate change vulnerability index for South African aquifers. Water SA 38(3):417–426. https://doi.org/10.10520/EJC121554

Ding Y, Zhang S, Zhao L, Li Z, Kang S (2019) Global warming weakening the inherent stability of glaciers and permafrost. Sci Bull 64(4):245–253. https://doi.org/10.1016/j.scib.2018.12.028

Engelbrecht CJ, Engelbrecht FA, Dyson LL (2013) High-resolution model-projected changes in mid-tropospheric closed-lows and extreme rainfall events over southern Africa. Int J Clim 33(1):173–187. https://doi.org/10.1002/joc.3420

Engelbrecht FA, Monteiro PMS (2021) The IPCC Assessment Report Six Working Group 1 report and southern Africa: reasons to take action. South Afr J Sci 117(11–12):1–7. https://doi.org/10.17159/sajs.2021/12679

Eyring V, Cox PM, Flato GM, Gleckler PJ, Abramowitz G, Caldwell P, Collins WD, Gier BK, Hall AD, Hoffman FM, Hurtt GC, Jahn A, Jones CD, Klein SA, Krasting JP, Kwiatkowski L, Lorenz R, Maloney E, Meehl GA et al (2019) Taking climate model evaluation to the next level. Nat Clim Change 9(2):Article 2. https://doi.org/10.1038/s41558-018-0355-y

Fowler HJ, Blenkinsop S, Tebaldi C (2007) Linking climate change modelling to impacts studies: recent advances in downscaling techniques for hydrological modelling. Int J Climatol 27(12):1547–1578. https://doi.org/10.1002/joc.1556

Gergis J, Henley BJ (2017) Southern hemisphere rainfall variability over the past 200 years. Clim Dyn 48(7):2087–2105. https://doi.org/10.1007/s00382-016-3191-7

Gidey E, Dikinya O, Sebego R, Segosebe E, Zenebe A (2018a) Predictions of future meteorological drought hazard (~ 2070) under the representative concentration path (RCP) 4.5 climate change scenarios in Raya, Northern Ethiopia. Model Earth Syst Environ 4(2):475–488. https://doi.org/10.1007/s40808-018-0453-x

Graham LP, Andersson L, Toucher MW, Wikner JJ, Wilk J (2022) Seasonal local rainfall and hydrological forecasting for Limpopo communities—a pragmatic approach. Clim Serv 27:100308. https://doi.org/10.1016/j.cliser.2022.100308

Gupta V, Singh V, Jain MK (2020) Assessment of precipitation extremes in India during the 21st century under SSP1–1.9 mitigation scenarios of CMIP6 GCMs. J Hydrol 590:125422. https://doi.org/10.1016/j.jhydrol.2020.125422

Hao Z, Singh VP, Xia Y (2018) Seasonal drought prediction: advances, challenges, and future prospects. Rev Geophys 56(1):108–141. https://doi.org/10.1002/2016RG000549

Harris I, Osborn TJ, Jones P, Lister D (2020) Version 4 of the CRU TS monthly high-resolution gridded multivariate climate dataset. Sci Data 7(1):1. https://doi.org/10.1038/s41597-020-0453-3

Hayes M, Svoboda M, Wall N, Widhalm M (2011) The Lincoln declaration on drought indices: universal meteorological drought index recommended. Bull Am Meteorol Soc 92(4):485–488

Huo-Po C, Jian-Qi S, Xiao-Li C (2013) Future changes of drought and flood events in china under a global warming scenario. Atmos Ocean Sci Lett 6(1):8–13. https://doi.org/10.1080/16742834.2013.11447051

Hurry L, Van Heerden J (1982) Southern Africa's weather patterns. Via Afrika

Iizumi T, Nishimori M, Dairaku K, Adachi SA, Yokozawa M (2011) Evaluation and intercomparison of downscaled daily precipitation indices over Japan in present-day climate: strengths and weaknesses of dynamical and bias correction-type statistical downscaling methods. J Geophys Res Atmos. https://doi.org/10.1029/2010JD014513

Kelley CP, Mohtadi S, Cane MA, Seager R, Kushnir Y (2015) Climate change in the Fertile Crescent and implications of the recent Syrian drought. Proc Natl Acad Sci 112(11):3241–3246. https://doi.org/10.1073/pnas.1421533112

Kruger AC, Shongwe S (2004) Temperature trends in South Africa: 1960–2003. Int J Clim 24(15):1929–1945. https://doi.org/10.1002/joc.1096

Kusangaya S, Mazvimavi D, Shekede MD, Masunga B, Kunedzimwe F, Manatsa D (2021) Climate change impact on hydrological regimes and extreme events in Southern Africa. In Diop S, Scheren P, Niang A (eds.) Climate change and water resources in Africa: perspectives and solutions towards an imminent water crisis (pp. 87–129). Springer International Publishing. https://doi.org/10.1007/978-3-030-61225-2_5

Kusangaya S, Warburton ML, Archer van Garderen E, Jewitt GPW (2014) Impacts of climate change on water resources in southern Africa: a review. Phys Chem Earth Parts A/B/C 67–69:47–54. https://doi.org/10.1016/j.pce.2013.09.014

Lange S, Volkholz J, Geiger T, Zhao F, Vega I, Veldkamp T, Reyer CPO, Warszawski L, Huber V, Jägermeyr J, Schewe J, Bresch DN, Büchner M, Chang J, Ciais P, Dury M, Emanuel K, Folberth C, Gerten D et al (2020) Projecting exposure to extreme climate impact events across six event categories and three spatial scales. Earth's Future 8(12):e2020EF001616. https://doi.org/10.1029/2020EF001616

Li Z, Chen Y, Li W, Deng H, Fang G (2015) Potential impacts of climate change on vegetation dynamics in Central Asia. J Geophys Res: Atmos 120(24):12345–12356. https://doi.org/10.1002/2015JD023618

Mann HB (1945) Nonparametric tests against trend. Econometrica 13(3):245–259. https://doi.org/10.2307/1907187

McKee TB, Doesken NJ, Kleist J (1993) The relationship of drought frequency and duration to time scales

Meehl GA, Boer GJ, Covey C, Latif M, Stouffer RJ (2000) The Coupled Model Intercomparison Project (CMIP). Bull Am Meteorol Soc 81(2):313–318

Mirgol B, Nazari M, Etedali HR, Zamanian K (2021) Past and future drought trends, duration, and frequency in the semi-arid Urmia Lake Basin under a changing climate. Meteorol Appl 28(4):e2009. https://doi.org/10.1002/met.2009

Mishra SS, Nagarajan R (2011) Spatio-temporal drought assessment in Tel river basin using Standardized Precipitation Index (SPI) and GIS. Geomat Nat Haz Risk 2(1):79–93. https://doi.org/10.1080/19475705.2010.533703

Mugejo K, Ncube B, Mutsvangwa C (2022) Infrastructure performance and irrigation water governance in Genadendal, Western Cape, South Africa. Sustainability 14(19):Article 19. https://doi.org/10.3390/su141912174

Mugido W, Shackleton CM (2017) The safety net function of NTFPs in different agro-ecological zones of South Africa. Popul Environ 39(1):107–125. https://doi.org/10.1007/s11111-017-0285-z

Muimba-Kankolongo A (2018) Food crop production by smallholder farmers in Southern Africa: challenges and opportunities for improvement. Academic Press, New York

Nam WH, Hayes MJ, Svoboda MD, Fuchs B, Tadesse T, Wilhite DA, Hong EM, Kim T (2017) Examining the extreme 2017 spring drought event in South Korea using a suite of drought indices (SPI, SC-PDSI, SPEI, EDI). 2017, H21F-1528

Ndebele NE, Grab S, Turasie A (2020) Characterizing rainfall in the south-western Cape, South Africa: 1841–2016. Int J Climatol 40(4):1992–2014. https://doi.org/10.1002/joc.6314

Ngwenya M, Gidey E, Simatele MD (2024) Agroecological-based modeling of meteorological drought at 12-month time scale in the Western Cape Province of South Africa. Earth Sci Inform. https://doi.org/10.1007/s12145-023-01193-3

O'Neill BC, Kriegler E, Ebi KL, Kemp-Benedict E, Riahi K, Rothman DS, van Ruijven BJ, van Vuuren DP, Birkmann J, Kok K, Levy M, Solecki W (2017) The roads ahead: narratives for shared socioeconomic pathways describing world futures in the 21st century. Glob Environ Change 42:169–180. https://doi.org/10.1016/j.gloenvcha.2015.01.004

Okunola OH, Simatele MD, Daramola O (2023) To live or to die: cultural and social factors influencing flood preparedness in Nigerian cities. Afr Geogr Rev 0(0):1–15. https://doi.org/10.1080/19376812.2023.2184841

Orimoloye IR, Ololade OO, Mazinyo SP, Kalumba AM, Ekundayo OY, Busayo ET, Akinsanola AA, Nel W (2019) Spatial assessment of drought severity in Cape Town area, South Africa. Heliyon 5(7):e02148. https://doi.org/10.1016/j.heliyon.2019.e02148

Otto FEL, Wolski P, Lehner F, Tebaldi C, van Oldenborgh GJ, Hogesteeger S, Singh R, Holden P, Fučkar NS, Odoulami RC, New M (2018) Anthropogenic influence on the drivers of the Western Cape drought 2015–2017. Environ Res Lett 13(12):124010. https://doi.org/10.1088/1748-9326/aae9f9

Palmer WC (1965) Meteorological drought. US Department of Commerce, Weather Bureau

Park C-K, Byun H-R, Deo R, Lee B-R (2015) Drought prediction till 2100 under RCP 8.5 climate change scenarios for Korea. J Hydrol 526:221–230. https://doi.org/10.1016/j.jhydrol.2014.10.043

Peng S, Wang C, Li Z, Mihara K, Kuramochi K, Toma Y, Hatano R (2023) Climate change multi-model projections in CMIP6 scenarios in Central Hokkaido, Japan. Sci Rep 13(1):Article 1. https://doi.org/10.1038/s41598-022-27357-7

Poornima S, Pushpalatha M (2019) Drought prediction based on SPI and SPEI with varying timescales using LSTM recurrent neural network. Soft Comput 23(18):8399–8412. https://doi.org/10.1007/s00500-019-04120-1

Qin J, Su B, Tao H, Wang Y, Huang J, Jiang T (2021) Projection of temperature and precipitation under SSPs-RCPs scenarios over northwest China. Front Earth Sci 15(1):23–37. https://doi.org/10.1007/s11707-020-0847-8

Rashid MdM, Beecham S, Chowdhury RK (2017) Simulation of extreme rainfall and projection of future changes using the GLIMCLIM model. Theor Appl Climatol 130(1):453–466. https://doi.org/10.1007/s00704-016-1892-9

Richardson CW (1981) Stochastic simulation of daily precipitation, temperature, and solar radiation. Water Resour Res 17(1):182–190. https://doi.org/10.1029/WR017i001p00182

Rogelj J, Meinshausen M, Knutti R (2012) Global warming under old and new scenarios using IPCC climate sensitivity range estimates. Nat Clim Change 2(4):Article 4. https://doi.org/10.1038/nclimate1385

Sachindra DA, Huang F, Barton A, Perera BJC (2014) Statistical downscaling of general circulation model outputs to precipitation—part 2: bias-correction and future projections. Int J Climatol 34(11):3282–3303. https://doi.org/10.1002/joc.3915

Salvi K, Kannan S, Ghosh S (2011) Statistical downscaling and bias-correction for projections of Indian rainfall and temperature in climate change studies. In 4th International Conference on Environmental and Computer Science 19:16–18

Sirdaş S, Sen Z (2003) Spatio-temporal drought analysis in the Trakya region, Turkey. Hydrol Sci J 48(5):809–820. https://doi.org/10.1623/hysj.48.5.809.51458

Sonali P, Nagesh Kumar D (2013) Review of trend detection methods and their application to detect temperature changes in India. J Hydrol 476:212–227. https://doi.org/10.1016/j.jhydrol.2012.10.034

Spinoni J, Barbosa P, Bucchignani E, Cassano J, Cavazos T, Christensen JH, Christensen OB, Coppola E, Evans J, Geyer B, Giorgi F, Hadjinicolaou P, Jacob D, Katzfey J, Koenigk T, Laprise R, Lennard CJ, Kurnaz ML, Li D et al (2020) Future global meteorological drought hot spots: a study based on CORDEX data. J Clim 33(9):3635–3661. https://doi.org/10.1175/JCLI-D-19-0084.1

Stefanidis S, Dafis S, Stathis D (2020) Evaluation of Regional Climate Models (RCMs) performance in simulating seasonal precipitation over Mountainous Central Pindus (Greece). Water 12(10):Article 10. https://doi.org/10.3390/w12102750

Svoboda M, Hayes M, Wood D (2012) Standardized Precipitation Index: user guide. Drought Mitigation Center Faculty Publications. https://digitalcommons.unl.edu/droughtfacpub/209

Tan ML, Duan Z (2017) Assessment of GPM and TRMM precipitation products over Singapore. Remote Sens 9(7):Article 7. https://doi.org/10.3390/rs9070720

Tapiador FJ, Navarro A, Moreno R, Sánchez JL, García-Ortega E (2020) Regional climate models: 30 years of dynamical downscaling. Atmos Res 235:104785. https://doi.org/10.1016/j.atmosres.2019.104785

Tebaldi C, Debeire K, Eyring V, Fischer E, Fyfe J, Friedlingstein P, Knutti R, Lowe J, O'Neill B, Sanderson B, van Vuuren D, Riahi K, Meinshausen M, Nicholls Z, Tokarska KB, Hurtt G, Kriegler E, Lamarque J-F, Meehl G et al (2021) Climate model projections from the Scenario Model Intercomparison Project (ScenarioMIP) of CMIP6. Earth Syst Dyn 12(1):253–293. https://doi.org/10.5194/esd-12-253-2021

Thomson AM, Calvin KV, Smith SJ, Kyle GP, Volke A, Patel P, Delgado-Arias S, Bond-Lamberty B, Wise MA, Clarke LE, Edmonds JA (2011) RCP4.5: a pathway for stabilization of radiative forcing by 2100. Clim Change 109(1):77. https://doi.org/10.1007/s10584-011-0151-4

Tyson PD (1986) Climatic change and variability in southern Africa. Cape Town: Oxford University Press

Um M-J, Kim Y, Jung K, Lee M, An H, Min I, Kwak J, Park D (2022) Evaluation of drought propagations with multiple indices in the

Yangtze River basin. J Environ Manag 317:115494. https://doi.org/10.1016/j.jenvman.2022.115494
Vicente-Serrano SM, Peña-Angulo D, Beguería S, Domínguez-Castro F, Tomás-Burguera M, Noguera I, Gimeno-Sotelo L, El Kenawy A (2022) Global drought trends and future projections. Philos Trans Roy Soc A Math Phys Eng Sci 380(2238):20210285. https://doi.org/10.1098/rsta.2021.0285
Vishwakarma A, Choudhary MK, Chauhan MS (2020) Applicability of SPI and RDI for forthcoming drought events: a non-parametric trend and one way ANOVA approach. J Water Clim Change 11(S1):18–28. https://doi.org/10.2166/wcc.2020.042
Wetherald RT, Manabe S (2002) Simulation of hydrologic changes associated with global warming. J Geophys Res Atmos 107(D19):ACL 7-1-ACL 7-15. https://doi.org/10.1029/2001JD001195
Zelinka MD, Myers TA, McCoy DT, Po-Chedley S, Caldwell PM, Ceppi P, Klein SA, Taylor KE (2020) Causes of higher climate sensitivity in CMIP6 models. Geophys Res Lett 47(1):e2019GL085782. https://doi.org/10.1029/2019GL085782
Zhang G, Su X, Ayantobo OO, Feng K (2021) Drought monitoring and evaluation using ESA CCI and GLDAS-Noah soil moisture datasets across China. Theor Appl Climatol 144(3):1407–1418. https://doi.org/10.1007/s00704-021-03609-w
Ziervogel G, Lennard C, Midgley G, New M, Simpson NP, Trisos CH, Zvobgo L (2022) Climate change in South Africa: risks and opportunities for climate-resilient development in the IPCC Sixth Assessment WGII Report. South Afr J Sci 118(9–10):1–5. https://doi.org/10.17159/sajs.2022/14492
Ziervogel G (2019) Unpacking the Cape Town drought: lessons learned. Cities support programme Climate resilience paper. African Centre for Cities, February